Application of a new vector mode solver to optical fiber-based plasmonic sensors

(Article begins on next page)

22 September 2024

APPLICATION OF A NEW VECTOR MODE SOLVER TO OPTICAL FIBER BASED PLASMONIC SENSORS

V. A. Popescu[1*] N. N. Puscas[1] G. Perrone[2]

[1]*Department of Physics, University Politehnica of Bucharest, Bucharest 060042 Romania*
[2]*Department of Electronics and Telecommunications, Politecnico di Torino, C.so Duca degli Abruzzi 24, I-10129 Torino, Italy*
*Corresponding author:vapopescu@yahoo.com

Our analytical method uses a linear combination of the Hankel functions H_1 and H_2 to represent the field in the gold region of a fiber based plasmonic sensor. This method is applied for different structures made from three, four and five layers. When the analyte is distilled water, the difference between the resonant wavelengths calculated with the finite element method and the analytical method is very small (0.00nm for three layers, 0.19nm for four layers and 0.07nm for five layers with two gold layers). The important characteristics of the Bessel and Hankel functions at the loss matching point are analysed.

Keywords: Sensors; surface plasmon resonance; finite element method; Numerical approximation and analysis

1. Introduction

A vector mode solver technique exploits the transfer matrix method, already applied for the analysis of planar waveguides[1] and optical fiber[2-5] to find the field distributions and propagation constants of the modes. The transfer matrix method has also been used to analysis and study the optical switching based on fiber grating[6-7]. The solution of the wave equation with cylindrical symmetry (the Debye potentials are parallel to the axis of rotation z) for electric field $\vec{E}$ and magnetic field $\vec{H}$ in the fiber yield to a dependency in the form $e^{-i\beta z}$ in the z direction and $e^{iv\varphi}$ around the circumference of the fiber, and to the radial solutions Ψ and Φ [3]:

$$\vec{E} = [(\frac{1}{r}\frac{\partial\Psi}{\partial\varphi} - \frac{\beta}{\omega\varepsilon_0 n^2}\frac{\partial\Phi}{\partial r})\vec{1}_r - (\frac{\partial\Psi}{\partial r} + \frac{\beta}{\omega\varepsilon_0 n^2 r}\frac{\partial\Phi}{\partial\varphi})\vec{1}_\varphi - (\frac{k^2 n^2 - \beta^2}{i\omega\varepsilon_0 n^2})\Phi\vec{1}_z]e^{-i\beta z}, \tag{1}$$

$$\vec{H} = [(\frac{1}{r}\frac{\partial\Phi}{\partial\varphi} + \frac{\beta}{\omega\mu_0}\frac{\partial\Psi}{\partial r})\vec{1}_r + (-\frac{\partial\Phi}{\partial r} + \frac{\beta}{\omega\mu_0 r}\frac{\partial\Psi}{\partial\varphi})\vec{1}_\varphi + (\frac{k^2 n^2 - \beta^2}{i\omega\mu_0})\Psi\vec{1}_z]e^{-i\beta z}, \tag{2}$$

where μ_0 is the free space magnetic permeability, ε_0 is the vacuum permittivity, ω is the angular frequency, $\vec{1}_r, \vec{1}_\varphi$ and $\vec{1}_z$ are the unit radial, tangential, and axial vectors and the mode index v must be an integer to ensure periodic solutions with period 2π. For a fiber with dielectric layers, the radial solutions Ψ and Φ are written as a combination of Bessel functions of the first kind (J) in the core layer, of Bessel functions of the first and second kinds (J and Y) in the dielectric interior clad layers, and of modified Bessel function of the second kind (K) in the outermost region. The continuity conditions require that the tangential components φ and z of the electric field E and the magnetic field H must be matched at the different layer interfaces.

In the paper by Dods[4], the layers of the fiber are lossless dielectric and thus only real propagation constants are considered. On the other hand, for a plasmonic sensor on the metal layers the refractive index is complex leading to complex propagation constants and to a modification in the field analytical expressions. In particular, in the proposed analytical method, the field in the gold region just before the outermost sensing region is represented in terms of a linear combination of the Hankel functions $H_1 = J + iY$ and $H_2 = J - iY$. The results of our simulations show that the propagation constants of different fiber structures are very close to those calculated with the finite element method.

2. Analytical method for plasmonic sensors

For a fiber structure with four layers, we have:

$$M_0\begin{pmatrix} A_1 \\ B_1 \\ C_1 \\ D_1 \end{pmatrix} = M_1\begin{pmatrix} A_2 \\ B_2 \\ C_2 \\ D_2 \end{pmatrix}; M_2\begin{pmatrix} A_2 \\ B_2 \\ C_2 \\ D_2 \end{pmatrix} = M_3\begin{pmatrix} A_3 \\ B_3 \\ C_3 \\ D_3 \end{pmatrix}; M_4\begin{pmatrix} A_3 \\ B_3 \\ C_3 \\ D_3 \end{pmatrix} = M_f\begin{pmatrix} A_4 \\ B_4 \\ C_4 \\ D_4 \end{pmatrix}, \tag{3}$$

where

$$M_0 = \begin{pmatrix} -\dfrac{u_1^2}{n_1^2}J_\nu(u_1 r_1) & 0 & 0 & 0 \\ -J_\nu^{'}(u_1 r_1) & 0 & \dfrac{i\nu\beta}{\omega\mu_0 r_1}J_\nu(u_1 r_1) & 0 \\ 0 & 0 & u_1^2 J_\nu(u_1 r_1) & 0 \\ -\dfrac{i\nu\beta}{\omega\varepsilon_0 n_1^2 r_1}J_\nu(u_1 r_1) & 0 & -J_\nu^{'}(u_1 r_1) & 0 \end{pmatrix}, \tag{4}$$

$$M_1 = \begin{pmatrix} -\dfrac{u_2^2}{n_2^2}J_\nu(u_2 r_1) & -\dfrac{u_2^2}{n_2^2}Y_\nu(u_2 r_1) & 0 & 0 \\ -J^{'}_\nu(u_2 r_1) & -Y^{'}_\nu(u_2 r_1) & \dfrac{i\nu\beta}{\omega\mu_0 r_1}J_\nu(u_2 r_1) & \dfrac{i\nu\beta}{\omega\mu_0 r_1}Y_\nu(u_2 r_1) \\ 0 & 0 & u_2^2 J_\nu(u_2 r_1) & u_2^2 Y_\nu(u_2 r_1) \\ -\dfrac{i\nu\beta}{\omega\varepsilon_0 n_2^2 r_1}J_\nu(u_2 r_1) & -\dfrac{i\nu\beta}{\omega\varepsilon_0 n_2^2 r_1}Y_\nu(u_2 r_1) & -J^{'}_\nu(u_2 r_1) & -Y^{'}_\nu(u_2 r_1) \end{pmatrix}, \tag{5}$$

$$M_2 = M_1(r_1 \rightarrow r_2) \tag{6}$$

$$M_3 = M_1(r_1 \rightarrow r_2, u_2 \rightarrow u_3, n_2 \rightarrow n_3, J_\nu \rightarrow H_{1\nu}, Y_\nu \rightarrow H_{2\nu}, J_\nu^{'} \rightarrow H_{1\nu}^{'}, Y_\nu^{'} \rightarrow H_{2\nu}^{'}) \tag{7}$$

$$M_4 = M_1(r_1 \rightarrow r_3, u_2 \rightarrow u_3, n_2 \rightarrow n_3, J_\nu \rightarrow H_{1\nu}, Y_\nu \rightarrow H_{2\nu}, J_\nu^{'} \rightarrow H_{1\nu}^{'}, Y_\nu^{'} \rightarrow H_{2\nu}^{'}) \tag{8}$$

$$M_f = \begin{pmatrix} 0 & \dfrac{w_4^2}{n_4^2}K_\nu(w_4 r_3) & 0 & 0 \\ 0 & -K_\nu^{'}(w_4 r_3) & 0 & \dfrac{i\nu\beta}{\omega\mu_0 r_3}K_\nu(w_4 r_3) \\ 0 & 0 & 0 & -w_4^2 K_\nu(w_4 r_3) \\ 0 & -\dfrac{i\nu\beta}{\omega\varepsilon_0 n_4^2 r_3}K_\nu(w_4 r_3) & 0 & -K_\nu^{'}(w_4 r_3) \end{pmatrix}, \tag{9}$$

$$u_1 = \sqrt{(kn_1)^2 - \beta^2}; u_2 = \sqrt{(kn_2)^2 - \beta^2}; u_3 = \sqrt{(kn_3)^2 - \beta^2}; w_4 = \sqrt{\beta^2 - (kn_4)^2}; \tag{10}$$

and where prime represents the differentiation with respect to the radial variable r:

$$F_\nu^{'}(u_i r_j) = \frac{u_i}{2}\{F_{\nu-1}(u_i r_j) - F_{\nu+1}(u_i r_j)\}, F = J, Y, H_1, H_2, \tag{11}$$

$$K_\nu^{'}(w_4 r_3) = \frac{w_4}{2}\{-K_{\nu-1}(w_4 r_3) - K_{\nu+1}(w_4 r_3)\} \tag{12}$$

The complex propagation constant $\beta = \beta_r + i\,\beta_i$, at a modal index ν is determined from the dispersion equation - the determinant (Δ) formed by the coefficients A_1, C_1, B_4 and D_4 of the equations

$$-\frac{u_1^2}{n_1^2}J_\nu(u_1 r_1)A_1 - B_{12\nu}B_4 - B_{14\nu}D_4 = 0, \tag{13}$$

$$-J'_\nu(u_1 r_1)A_1 + \frac{i\nu\beta}{\omega\mu_0 r_1}J_\nu(u_1 r_1)C_1 - B_{22\nu}B_4 - B_{24\nu}D_4 = 0, \tag{14}$$

$$u_1{}^2 J_\nu(u_1 r_1)C_1 - B_{32\nu}B_4 - B_{34\nu}D_4 = 0, \tag{15}$$

$$-\frac{i\nu\beta}{\omega\varepsilon_0 n_1{}^2 r_1}J_\nu(u_1 r_1)A_1 - J'_\nu(u_1 r_1)C_1 - B_{42\nu}B_4 - B_{44\nu}D_4 = 0, \tag{16}$$

must vanish:

$$\Delta = 0, \tag{17}$$

where

$$\Delta = \begin{vmatrix} -\dfrac{u_1{}^2}{n_1{}^2}J_\nu(u_1 r_1) & 0 & -B_{12\nu} & -B_{14\nu} \\[2mm] -J'_\nu(u_1 r_1) & \dfrac{i\nu\beta}{\omega\mu_0 r_1}J_\nu(u_1 r_1) & -B_{22\nu} & -B_{24\nu} \\[2mm] 0 & u_1{}^2 J_\nu(u_1 r_1) & -B_{32\nu} & -B_{34\nu} \\[2mm] -\dfrac{i\nu\beta}{\omega\varepsilon_0 n_1{}^2 r_1}J_\nu(u_1 r_1) & -J'_\nu(u_1 r_1) & -B_{42\nu} & -B_{44\nu} \end{vmatrix} \tag{18}$$

$$M_1 M_2{}^{-1} M_3 M_4{}^{-1} M_f = B_\nu, \tag{19}$$

$$B_\nu = \begin{pmatrix} 0 & B_{12\nu} & 0 & B_{14\nu} \\ 0 & B_{22\nu} & 0 & B_{24\nu} \\ 0 & B_{32\nu} & 0 & B_{34\nu} \\ 0 & B_{42\nu} & 0 & B_{44\nu} \end{pmatrix} \tag{20}$$

Similarly, for a fiber structure with five layers, we have:

$$M_0\begin{pmatrix}A_1\\B_1\\C_1\\D_1\end{pmatrix} = M_1\begin{pmatrix}A_2\\B_2\\C_2\\D_2\end{pmatrix}; M_2\begin{pmatrix}A_2\\B_2\\C_2\\D_2\end{pmatrix} = M_3\begin{pmatrix}A_3\\B_3\\C_3\\D_3\end{pmatrix}; M_4\begin{pmatrix}A_3\\B_3\\C_3\\D_3\end{pmatrix} = M_5\begin{pmatrix}A_4\\B_4\\C_4\\D_4\end{pmatrix}; M_6\begin{pmatrix}A_4\\B_4\\C_4\\D_4\end{pmatrix} = M_f\begin{pmatrix}A_5\\B_5\\C_5\\D_5\end{pmatrix}, \tag{21}$$

where M_0, M_1 and M_2 are the same as for the fiber with four layers and M_3, M_4, M_5, M_6 and M_f can be obtained from the corresponding relations (7)-(9):

$$M_3 = M_3(H_{1\nu} \to J_\nu, H_{2\nu} \to Y_\nu, H'_{1\nu} \to J'_\nu, H'_{2\nu} \to Y'_\nu), \tag{7'}$$

$$M_4 = M_4(H_{1\nu} \to J_\nu, H_{2\nu} \to Y_\nu, H'_{1\nu} \to J'_\nu, H'_{2\nu} \to Y'_\nu), \tag{8'}$$

$$M_5 = M_3(r_2 \to r_3, u_3 \to u_4, n_3 \to n_4), \tag{7''}$$

$$M_6 = M_4(r_3 \to r_4, u_3 \to u_4, n_3 \to n_4), \tag{8''}$$

$$M_f = M_f(r_3 \to r_4, w_4 \to w_5, n_4 \to n_5) \tag{9'}$$

and

$$u_1 = \sqrt{(kn_1)^2 - \beta^2}; u_2 = \sqrt{(kn_2)^2 - \beta^2}; u_3 = \sqrt{(kn_3)^2 - \beta^2}; u_4 = \sqrt{(kn_4)^2 - \beta^2}; \tag{22}$$

$$w_5 = \sqrt{(\beta)^2 - (kn_5)^2}, \tag{23}$$

The complex propagation constant is determined from a similar dispersion equation (17) as for a fiber with four layers, but the determinant is formed by the coefficients A_1, C_1, B_5 and D_5 of the corresponding equations and

$$M_1 M_2{}^{-1} M_3 M_4{}^{-1} M_5 M_6{}^{-1} M_f = B_\nu, \tag{24}$$

For a fiber structure with five layers and with two gold layers[3], we must to replace M_1 and M_2 from (5) and (6) with the following relations

$$M_1 = M_1(J_\nu \to H_{1\nu}, Y_\nu \to H_{2\nu}, J'_\nu \to H'_{1\nu}, Y'_\nu \to H'_{2\nu}), \tag{25}$$

$$M_2 = M_2(J_\nu \to H_{1\nu}, Y_\nu \to H_{2\nu}, J'_\nu \to H'_{1\nu}, Y'_\nu \to H'_{2\nu}), \tag{26}$$

In general, for a fiber with N layers there is a number of N-2 pair of the products of the form $M_i M_{i+1}{}^{-1}$.

3. Numerical results and discussion

The method is demonstrated in a fiber based plasmonic sensor considering a simplified fiber structure which is made by a SiO_2 core in the center of the structure, surrounded by a thin inner GaP layer, a gold reflector layer and a water-based analyte layer (Fig. 1). This method is used to compute the propagation constants of the core and plasmon modes in the structure. The wavelength dependence of the refractive index of silica[8-10], distilled water[11], gold[8-9,12], heavy water[13] and GaP[14] has been modeled by using, respectively, a Sellmeier formula for SiO_2, GaP, H_2O and D_2O and a Drude relation for Au.

The proposed analytical method has been validated by comparison with the results obtained with a finite elements analysis. First we considered a fiber with four layers, similar to the case shown in Fig.1, with all-real and all-real but the gold layer refractive indices. For both cases the radii defining the various layers are $r_1 = 1.527$ μm, $r_2 = 1.567$ μm, $r_3 = 1.587$ μm, while the refractive index at the wavelength of 0.85 μm are $n_1 = 1.4488$, $n_2 = 1.444$, $n_4 = 1$. In the all-real indices case, the "plasmonic" layer located before the outermost clad region is supposed to be a layer loaded with nano particle gold resulting in a real refractive index $n_3 = 1.42$. In this case we use the Bessel functions J and Y instead of the Hankel functions H_1 and H_2 to express the field in the nano particle gold layer. The values of the effective index for HE_{11}, TE_{01} and TM_{01} modes, calculated with the analytical method (respectively, 1.435774, 1.416931, 1.414350) resulted very close to those obtained with the finite element method (respectively, 1.435771, 1.416934, 1.414350). Note that, using a linear combination of K and H_1 functions (as in[13-14] but with smaller operating dimensions) instead of J and Y functions, the results computed with the analytical and numerical methods are different. As for the other case, always assuming a 20 nm thick "plasmonic" layer, but this time of pure gold, we have at 0.85 μm $n_3 = 0.243806 + 4.934597i$. Again, the values of the effective index for HE_{11}, TE_{01} and TM_{01} modes calculated with the analytical method – this time using Hankel functions – (respectively, 1.432349 + 0.000285i, 1.412215 + 0.000099i, 1.401919 + 0.001195i) are very close to those found using the finite element method (respectively, 1.432350 + 0.000285i, 1.412236 + 0.000098i, 1.401922 + 0.001194i). Similar comparisons have been carried out also for fiber structures having a different number of layers, from three to five. For an optical fiber with four (SiO_2, GaP, gold and distilled water) layers ($r_1 = 1.527$ μm, $r_2 = 1.567$ μm, $r_3 = 1.607$ μm) at the loss matching point ($\lambda = 0.62909$ μm) computed with the finite element method, the effective index computed with the finite element method for the core

(1.449802 + 0.003563i) and plasmon (1.446495 + 0.003564i) modes are very close to those found using the analytical method (1.449702 + 0.003610i for the core mode and 1.446494 + 0.003490i for the plasmon mode). For an optical fiber with three (SiO_2, gold and distilled water) layers (r_1 = 1.527 μm, r_2 = 1.567 μm) at the loss matching point (λ = 0.5655 μm) computed with the finite element method[17], the effective index computed with the finite element method for the core (1.447994 + 0.001979i) and plasmon (1.455284 + 0.001987i) modes are very close to those found using the analytical method (1.447990 + 0.001982i for the core mode and 1.455276 + 0.001985i for the plasmon mode). For an optical fiber with five (SiO_2, gold, SiO_2, gold and distilled water) layers (r_1 = 9 μm, r_2 = 0.94 μm, r_3 = 1.527 μm, r_4 = 1.567 μm) at the loss matching point (λ = 0.6057 μm) computed with the finite element method[16], the effective index computed with the finite element method for the core (1.427842 + 0.002221i) and plasmon (1.431005 + 0.002227i) modes are very close to those found using the analytical method (1.427837 + 0.002214i for the core mode and 1.430997 + 0.002233i for the plasmon mode). In all the cases the difference between the calculated values with the finite element method and analytical method is very small, hence demonstrating the correctness of the analytical implementation.

After having validating the approach, we used the analytical and finite element methods to study a sensor with only four layers. The device is made of SiO_2 core (r_1= 1.527 μm) surrounded by a GaP layer (thickness r_2 − r_1 = 40 nm) and a gold layer (thickness r_3 − r_2 = 40 nm); according to the finite element analysis, the difference between the imaginary parts of the effective indices of core and plasmon modes is the smallest (0.000001) at the loss matching point (λ = 0.62909 μm) where β/k = 1.449802 + 0.003563i for the core mode and β/k = 1.446495 + 0.003564i for the plasmon mode when the analyte is pure distilled water. Then, the resonance shifts to λ = 0.61576 μm when the analyte is heavy water. When the analyte is distilled water, the effective indices of the core and plasmon modes at the loss matching point (λ = 0.62928 μm) calculated with the analytical method are β/k = 1.446444 + 0.003547i and β/k = 1.449672 + 0.003549i, respectively. The difference between the resonant wavelengths calculated with the finite element method and analytical method is only 0.19 nm. When the analyte is heavy water, the effective indices of the core and plasmon modes at the loss matching point (λ = 0.61581 μm) calculated with the analytical method are β/k = 1.450399 + 0.003591i and β/k = 1.447580 + 0.003592i, respectively. The difference between the resonant wavelengths calculated with the finite element method and analytical method is only 0.05 nm. Fig. 2 reports the real and imaginary parts of the determinant Δ corresponding to the dispersion equation versus the real part of the effective index for HE_{11} core and plasmon modes near the loss matching point when the analyte is heavy water for a fiber with four layers. Fig. 3 reports the same characteristics when the analyte is distilled water for a fiber with three layers. Figs. 2 and 3 show that the exact values of the real part of the effective index for the core and plasmon modes are between the intersections of the real and imaginary parts of the determinant Δ corresponding to the dispersion equation with the real part of β/k.

Fig. 4 shows the real and imaginary parts of the Bessel function J in the core layer, modified Bessel function K in the analyte layer and Hankel functions H_1 and H_2 in the gold layer at the loss matching point (λ = 0.61576 μm) of the core mode HE_{11} when the analyte is heavy water for a fiber with four layers. It is interesting to note that the real and imaginary parts of the functions J and H have opposite variations and when the imaginary part of the J function in the core layer is zero, the real part of J is maximum. The values of the function K in the analytical layer are small and to a decrease of the real part corresponds an increase of the

imaginary part. Although the values of the Hankel function H_1 are very small and the values of the Hankel function H_2 are very large, the elements of the matrix M_3 and M_4^{-1} are also very small or very large, but the elements of the product $M_3M_4^{-1}$ are small. To exemplify we give only the first elements of these matrices:

$M_3(1,1) = (-1.84807+4.79725i)\times10^{-26}$, $M_3(1,2) = (-2.87089+0.930032i)\times10^{27}$, $M_3(1,3) = 0$, $M_3(1,4) = 0$, $M_4^{-1}(1,1) = (-1.86522-4.21372i)\times10^{25}$, $M_4^{-1}(1,2) = (5.31849+13.5692i)\times10^{25}$, $M_4^{-1}(1,3) = (-22.0509+7.01964i)\times10^{19}$, $M_4^{-1}(1,4) = 0$, $M_3M_4^{-1}(1,1) = 2.47432-0.110813i$, $M_3M_4^{-1}(1,2) = -7.15737+0.0747071i$, $M_3M_4^{-1}(1,3) = (6.23832-11.348i)\times10^{-7}$, $M_3M_4^{-1}(1,4) = 0$.

Fig. 5 shows the real and imaginary parts of the Bessel functions J and Y in GaP layer at the loss matching point ($\lambda = 0.61576$ µm) of the core mode HE_{11} when the analyte is heavy water for a fiber with four layers. It is interesting to note that in the GaP layer, the imaginary part $Im(J)$ of the functions J is maximum when the real part $Re(J)$ of J is zero. Also, the real part of the functions Y is maximum when the imaginary part of Y is zero and $Re(J)$ and $Im(Y)$ have an opposite linear variation. In our case of complex arguments, these functions show features of oscillating and exponential type functions. There is a balance between the real and imaginary parts of the complex functions J and Y at a fixed value of the resonant wavelength.

Our analytical method is also applied to a structure with three and five layers when the analyte is distilled water. For a fiber with three layers ($r_1 = 1.527$ µm, $r_2 = 1.567$ µm), the effective index of the core and plasmon modes at the loss matching point ($\lambda = 0.5655$ µm) calculated with the analytical method are $\beta/k = 1.447990 + 0.001982i$ and $\beta/k = 1.455276 + 0.001985i$, respectively. The difference between the resonant wavelengths calculated with the finite element method[17] and analytical method is 0.00 nm. For a fiber structure with five layers and with two gold layers[18], the effective index of the core and plasmon modes at the loss matching point ($\lambda = 0.60577$ µm) calculated with the analytical method are $\beta/k = 1.427816 + 0.002223i$ and $\beta/k = 1.430982 + 0.002224i$, respectively. The difference between the resonant wavelengths calculated with the finite element method and analytical method is only 0.07nm.

The results computed with the numerical finite element method are not very close to those calculated with the analytical method for high contrast of the refractive index or if one domain (in the nanometer range) is not large enough. In this case very fine meshes are required to obtain reasonable numerical solutions[19].

4. Conclusions

In the proposed analytical method, a linear combination of the Hankel functions H_1 and H_2 is used to represent the field in the gold region, just before the outermost sensing region, of fiber-based plasmonic sensors. Our results for different fiber structures are very close to those calculated with the finite element method. The most important characteristics of the Bessel and Hankel functions at the resonant wavelength of the core mode HE_{11} for a fiber with four layers are analysed. One advantage of our analytical method is that can also be used for high contrast (refractive index or thickness) problems.

REFERENCES

1. J. Chilwell and I. Hodgkinson, *J. Opt. Soc. Am. A* **1**, (1984) 742

2. C. Yeh and G. Lindgren, *Applied Optics* **16** (1977) 483

3. C. Y. H. Tsao, *J. Opt. Soc. Am. A* **6** (1989) 555

4. S. R. Dods, *Integrated Photonics Research and Applications (IPRA) Technical Digest* ITuF5 (2006) **ITuF**

5. V. A. Popescu, *J. Supercond. Nov. Magn.* **25** (2012) 1413

6. Z. Zang, *Applied Optics* **52** (2013) 5701

7. Z. Zang and Y. Zhang, *Applied Optics* **51** (2012) 3424

8. A. K. Sharma, Rajan and R. B. D.Gupta, *Opt. Commun.* **274** (2007) 320

9. R. K. Verma, A. K. Sharma and B. D.Gupta, *Opt. Commun.* **281** (2008) 1486

10. A. K. Ghatak and K. Thyagarajan, *Introduction to Fiber Optics* (Cambridge University Press, 1999)

11. M. Daimon and A. Masumura, *Appl. Opt.* **46** (2007) 3811

12. M. A. Ordal, L. L. Long, R. J. Bell, S. E. Bell, R. R. Bell, R. W. Alexander Jr. and C.A. Ward, *Appl. Opt.* **22** (1983) 1099

13. H. Odhner and D. T. Jacobs, *J. Chem. Eng. Data* **57** (2012) 166

14. F. L. Madarasz, J. O. Dimmock, N. Dietz and K. L. Bachmann, *J. Appl. Phys.* **87** (2000) 1564

15 P. K. Choudhury, *Adv. Mater. Scieng.* **214614** (2012) 1

16 F. A. Rahman, P. K. Choudhury, D. Kumar and Z. Yusoff, *Prog. Electromagn. Res.* **PIER 90** (2009) 209

17. P. Dhara, C. Fallauto, A. Braglia, M. Olivero, V. A. Popescu, N. N. Puscas, A. Vallan, V. K. Singh, G. Perrone, in *Optical Fibers and Sensors for Medical Diagnostics and Treatment Applications XV*, I. Gannot, ed., Proc. SPIE **9317** (2015) 1

18. V. A. Popescu, N. N. Puscas and G. Perrone, *J. Opt. Soc. Am. B* **32** (2015) 473

19. S. Ham and K.-J. Bathe, *Comput. Struct.* **94-95** (2012) 1

Figure Captions

Fig.1. Cross section of an optical fiber with four layers made by SiO_2 core (radius r_1) surrounded by a GaP layer (thickness $r_2 - r_1$), a gold layer (thickness $r_3 - r_2$ and by a water layer which can be considered infinite for the numerical model.

Fig. 2. The real (solid line) and imaginary (dashed line) parts of the determinant Δ corresponding to the dispersion equation versus the real part of the effective index for HE_{11} core and plasmon modes near the loss matching point ($\lambda = 0.61581$ μm) when the analyte is heavy water for a fiber with four layers.

Fig. 3. The real (solid line) and imaginary (dashed line) parts of the determinant Δ corresponding to the dispersion equation versus the real part of the effective index for HE_{11} core and plasmon modes near the loss matching point ($\lambda = 0.5655$ μm) when the analyte is distilled water for a fiber with three layers.

Fig. 4. The real and imaginary parts of the Bessel function J in the core layer (a), modified Bessel function K in the analytical layer (b) and Hankel functions H_1 in (c) and H_2 in (d) in the gold layer at the loss matching point ($\lambda = 0.61576$ μm) of the core mode HE_{11} when the analyte is heavy water for a fiber with four layers.

Fig. 5. The real and imaginary parts of the Bessel functions J in (a) and (b) and Y in (c) and (d) in GaP layer at the loss matching point ($\lambda = 0.61576$ μm) of the core mode HE_{11} when the analyte is heavy water for a fiber with four layers.
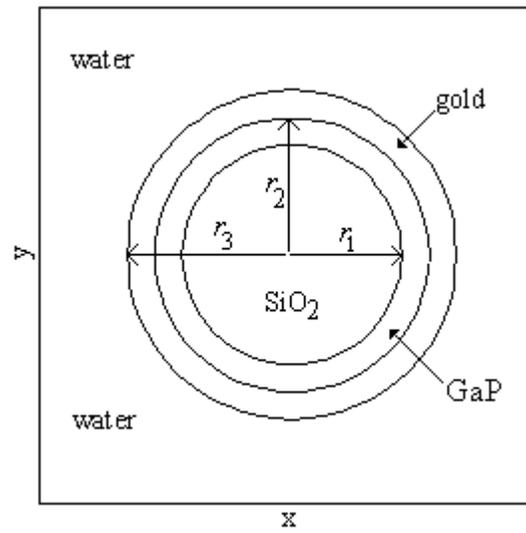
Fig.1. Cross section of an optical fiber with four layers made by SiO_2 core (radius r_1) surrounded by a GaP layer (thickness $r_2 - r_1$), a gold layer (thickness $r_3 - r_2$ and by a water layer which can be considered infinite for the numerical model.
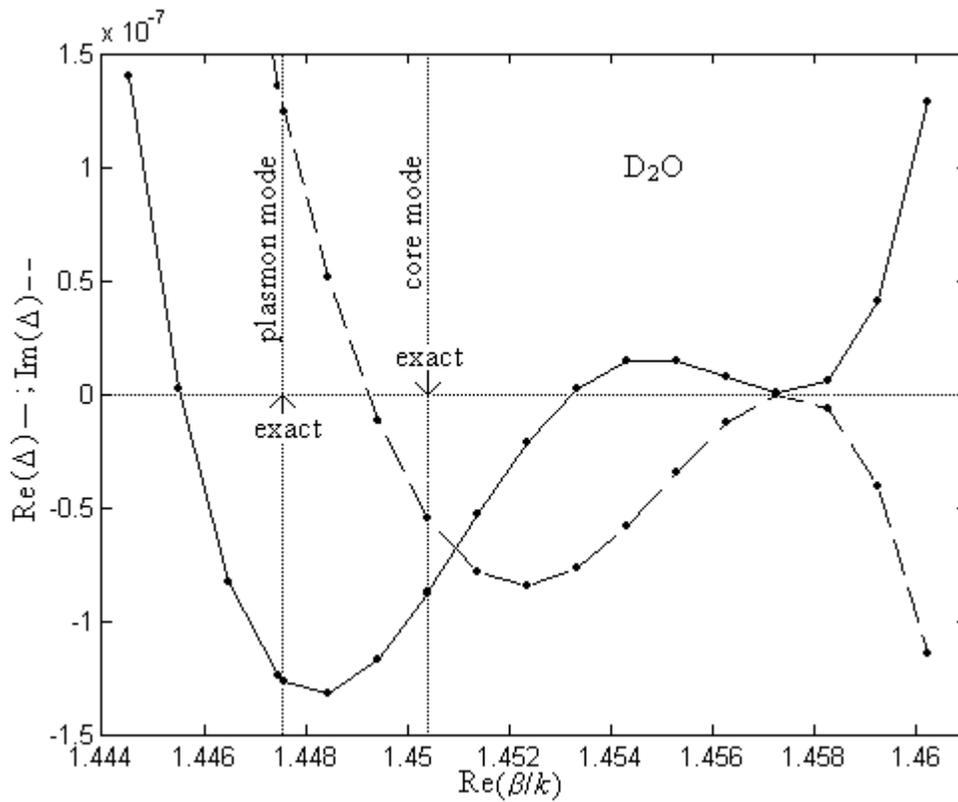
Fig. 2. The real (solid line) and imaginary (dashed line) parts of the determinant Δ corresponding to the dispersion equation versus the real part of the effective index for HE_{11} core and plasmon modes near the loss matching point ($\lambda = 0.61581$ μm) when the analyte is heavy water for a fiber with four layers.
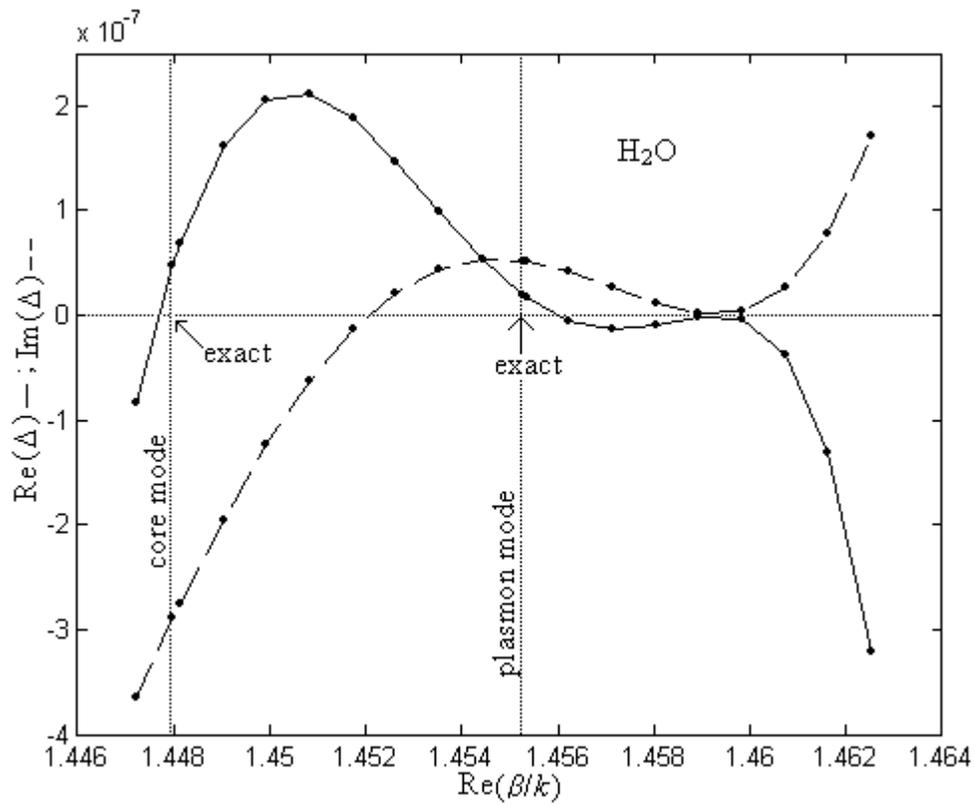
Fig. 3. The real (solid line) and imaginary (dashed line) parts of the determinant Δ corresponding to the dispersion equation versus the real part of the effective index for HE_{11} core and plasmon modes near the loss matching point ($\lambda = 0.5655$ μm) when the analyte is distilled water for a fiber with three layers.
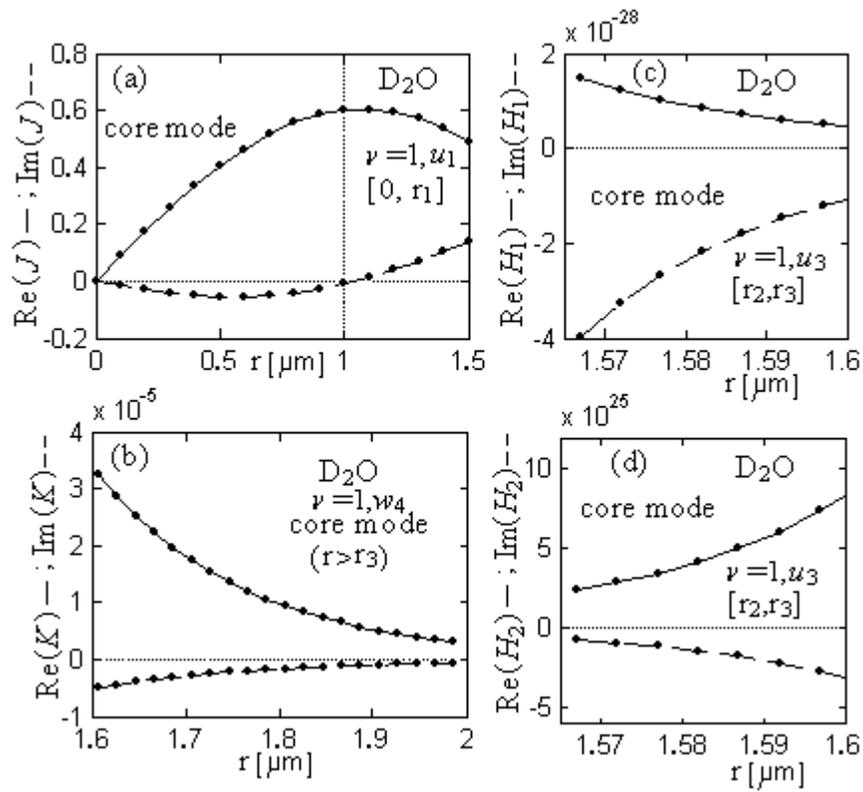
Fig. 4. The real and imaginary parts of the Bessel function J in the core layer (a), modified Bessel function K in the analytical layer (b) and Hankel functions H_1 in (c) and H_2 in (d) in the gold layer at the loss matching point ($\lambda = 0.61576$ μm) of the core mode HE_{11} when the analyte is heavy water for a fiber with four layers.
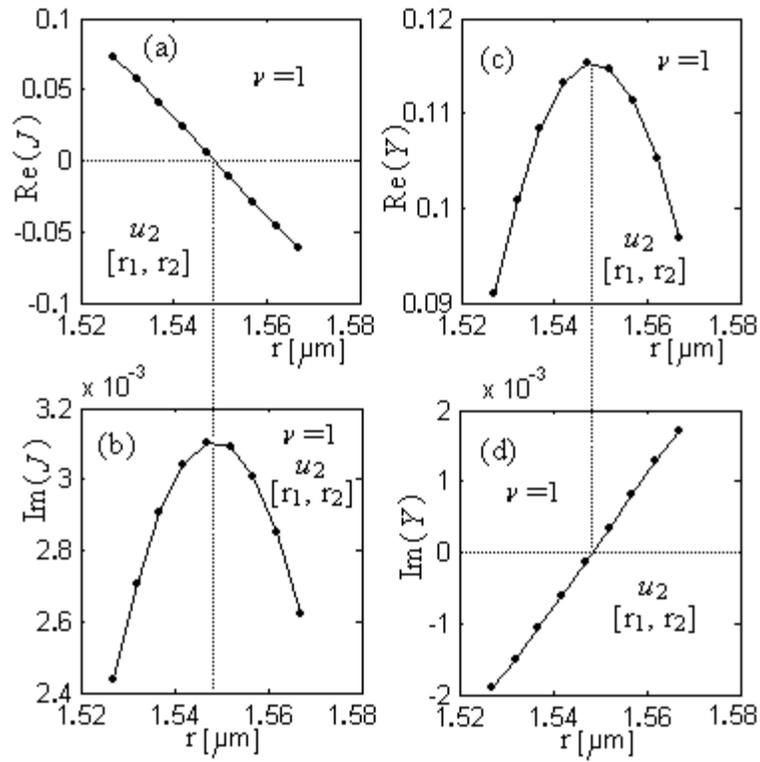
Fig. 5. The real and imaginary parts of the Bessel functions J in (a) and (b) and Y in (c) and (d) in GaP layer at the loss matching point ($\lambda = 0.61576$ μm) of the core mode HE_{11} when the analyte is heavy water for a fiber with four layers.